BJRS
BRAZILIAN JOURNAL OF RADIATION SCIENCES

doi.org/10.15392/2319-0612.2025.2940
Braz. J. Radiat. Sci., Rio de Janeiro
2025, 13(4) | 01-20 | e2940
Editor: Prof. Dr. Bernardo Maranhão Dantas
Editor: Prof. Dr. Alfredo Lopes Ferreira Filho
Submitted: 2025-05-19
Accepted: 2025-08-06

Development of a semi-analytical nodal methodology for one-dimensional eigenvalue problems based on multigroup neutron transport theory using the discrete ordinate formulation

Pinheiro[a,b*], N. R.; Oliveira[a], F. B. S.; Alves Filho[b], H.

[a] Santa Cruz State University, Soane Nazaré de Andrade Campus, Ilhéus, BA, Brazil.
[b] State University of Rio de Janeiro, Polytechnic Institute, Nova Friburgo, RJ, Brazil.

*Correspondence: nrpinheiro@uesc.br

Abstract: A semi-analytical nodal methodology is described in this paper for obtaining the numerical solution of eigenvalue problems based on neutron transport theory, in slab geometry, with isotropic scattering, using the discrete ordinates and multigroup energy formulation. This new approach applies a quadratic polynomial approximation only to the fission term in the transport equation, which justifies the method being classified as semi-analytical. The numerical solution is obtained through two interconnected iterative processes: the outer iterative process, which uses the power method to obtain successive estimates for the fission source and the effective multiplication factor (k_{eff}), and the internal iterative process, which aims to obtain successive estimates of the angular neutron fluxes emerging from the homogeneous regions throughout the spatial domain. Once the eigenvalues are calculated, for each outer power iteration, the angular fluxes of neutrons emerging at the node faces and in the sweeping direction of the internal iterative process are estimated. These are incoming fluxes at the faces of adjacent nodes, which ensures the continuity of the numerical solution. Computational algorithms were implemented in MATLAB. Numerical results for a typical benchmark problem considering an ADS, c.f., Accelerator-Driven Subcritical Reactor, type model are provided to illustrate the accuracy of the converged numerical solutions in coarse-mesh calculations. Although the method is not free from spatial truncation error, the results for the benchmark problem were considered satisfactory with one node per region, and refining the spatial domain did not result in a high computational cost in terms of response time, with results approaching those of analytical solutions.

Keywords: Neutron transport equation, Multigroup energy formulation, Nodal methodology, Quadratic approximation.

BJRS
BRAZILIAN JOURNAL OF RADIATION SCIENCES

doi.org/10.15392/2319-0612.2025.2940
Braz. J. Radiat. Sci., Rio de Janeiro
2025, 13(4) | 01-20 | e2940
Editor: Prof. Dr. Bernardo Maranhão Dantas
Editor: Prof. Dr. Alfredo Lopes Ferreira Filho
Submitted: 2025-05-19
Accepted: 2025-08-06

Desenvolvimento de uma metodologia nodal semi-analítica para problemas unidimensionais de autovalor baseado na teoria de transporte multigrupo de nêutrons usando a formulação das ordenadas discretas

Resumo: Uma metodologia nodal semi-analítica é descrita neste artigo para a obtenção da solução numérica de problemas de autovalor baseada na teoria de transporte de nêutrons, em geometria slab, com espalhamento isotrópico, usando a formulação das ordenadas discretas e multigrupo de energia. Esta nova proposta faz uma aproximação polinomial quadrática apenas no termo de fissão da equação de transporte, o que justifica o método ser semi-analítico. A solução numérica é obtida por meio de dois processos iterativos interligados: o processo iterativo externo, que utiliza o método das potências para obter sucessivas estimativas para a fonte de fissão e o fator de multiplicação efetivo (k_{eff}), e o processo iterativo interno, que visa obter sucessivas estimativas dos fluxos angulares de nêutrons emergentes das regiões homogêneas em todo domínio espacial. Uma vez calculados os autovalores, para cada iteração externa de potência estima-se os fluxos angulares emergentes nas faces dos nodos e na direção da varredura do processo iterativo interno. Estes são os fluxos incidentes nas faces dos nodos adjacentes, o que garante a continuidade da solução numérica. Os algoritmos computacionais foram implementados em linguagem MATLAB. Resultados numéricos para um problema de benchmark típico, considerando um modelo do tipo ADS, c.f., Accelerator-Driven Subcritical Reactor, são fornecidos para ilustrar a precisão das soluções numéricas convergidas em cálculos de malha grossa. Apesar do método não ser livre de erro de truncamento espacial, os resultados do problema de benchmark foram considerados satisfatórios com um nodo por região e o refinamento do domínio espacial não demandou alto custo computacional no que tange o tempo de resposta, aproximando seus resultados aos das soluções analíticas.

Palavras-chave: Equação de transporte de nêutrons, Formulação multigrupo de energia, Metodologia nodal, Aproximação quadrática.

1. INTRODUCTION

Traditional deterministic numerical methods, whether fine-mesh (Diamond Difference method) [1], or coarse-mesh (nodal methods) [2,3], play a fundamental role in the calculations of the effective multiplication factor (k_{eff}) and the power distribution in a nuclear reactor.

Barros and Larsen [4] developed a spectronodal (coarse-mesh) method for neutron shielding problems (fixed-source) where, in one-dimensional calculations, the scattering and fission terms of the intranodal S_N equations were treated without approximations. The method was called SGF, c.f., Spectral Green´s Function. The iterative scheme NBI [4], c.f., One-Node Block Inversion, used in the internal iterations of the iterative process, was also developed and presented, and its results were compared with the traditional SI scheme, cf. Source Iteration [1]. The NBI scheme, despite being more expensive from the point of view of computational memory, presents a higher convergence speed than the SI scheme in coarse mesh calculations.

Abreu [5] developed a spectronodal method which was applied to neutron criticality (eigenvalue) problems, considering one-dimensional spatial domains and multigroup energy formulation. The method was called SD-SGF, c.f., spectral diamond-spectral Green's function, and represented a significant advance in the development of this type of numerical approach.

Recently, Ramirez [6], following this same approach, proposed two spectronodal methodologies that were tested in criticality problems. The Analytical Spectral-Nodal Method (ASNM) and Analytical Spectral-Nodal Method-Source Iteration (ASNM-SI) methods were developed. The numerical results obtained with these methods were compared with the DD method [1] and the SD-SGF method [5].

In this paper, we present and develop a new nodal methodology, which makes a quadratic polynomial approximation in the fission term and considers the scattering term without approximations in global nuclear reactor problems, considering one-dimensional spatial domains. The numerical results were compared with the results obtained by the DD fine-mesh method. We obtained satisfactory results for 1 node per region, and the refinement did not demand high computational cost in terms of response time. This paper was divided as follows: in section 2, the entire mathematical modeling of the proposed methodology is developed, in section 3 the numerical results of the model-problem considered are presented and in section 4 the final considerations and future perspectives are presented.

2. SEMI-ANALYTICAL NODAL METHODOLOGY

2.1. Mathematical modeling

The equation that models neutron transport in a one-dimensional domain D of length H (Fig. 1), in slab geometry, stationary condition, with isotropic scattering, in multiplicative media, in the discrete ordinate formulation S_N and in the multigroup energy formulation is given by

$$\begin{aligned}\mu_m \frac{d}{dx}\psi_{g,m}(x) + \sigma_{t,g}(x)\psi_{g,m}(x) &= \frac{\chi_g}{2k_{eff}} \sum_{g'=1}^{G} \nu\sigma_{fg'}(x) \sum_{n=1}^{N} \omega_n \psi_{g',n}(x) \\ &+ \frac{1}{2} \sum_{g'=1}^{G} \sigma_s^{g'\to g}(x) \sum_{n=1}^{N} \omega_n \psi_{g',n}(x),\end{aligned} \tag{1}$$

with $m = 1{:}\,N$, $g = 1{:}\,G$ and $0 \le x \le H$, where $\psi_{g,m}(x) \equiv \psi_g(x, \mu_m)$.

In Equation (1), the dependent variable $\psi_{g,m}(x)$ represents the angular neutron flux. The discrete values μ_m are the roots of the Legendre polynomials of degree N, the quadrature weights ω_n are such that they exactly integrate the Legendre polynomials of degree 0 to N-1, $\sigma_{t,g}(x)$, $\sigma_{fg}(x)$, and $\sigma_s^{g'\to g}(x)$ are, respectively, the total cross section, the fission cross section, and the scattering cross section, k_{eff} is the effective multiplication factor, χ_g is the fission spectrum, and ν is the average number of fast neutrons produced per fission.

The boundary conditions used are of the vacuum type and, for $g = 1{:}\,G$, take the form

$$\begin{cases} \psi_{g,m}(0) = 0, & m = 1{:}\,N/2\,, \\ \psi_{g,m}(H) = 0, & m = (N/2+1){:}\,N. \end{cases} \tag{2}$$

2.2. Discretization of the spatial domain

The discretization of the spatial domain consists of dividing the domain D (Fig. **11111**) into a number J of spatial regions (or nodes) Γ_j, $j = 1{:}\,J$, with dimensions $h_j = x_{j+1/2} - x_{j-1/2}$, where the nuclear parameters are uniform.

Figure 1: Spatial grid in a one-dimensional domain D of length H cm.

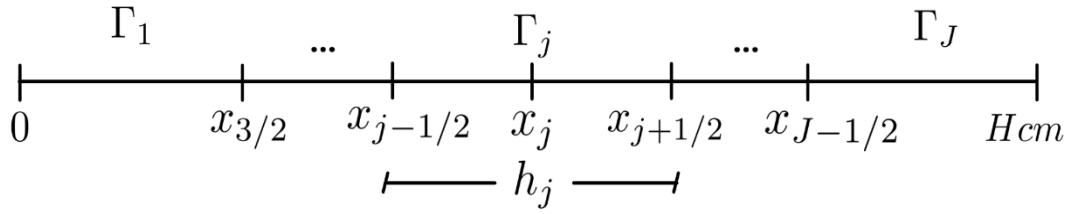

Thus, in each homogeneous region Γ_j, Eq. (1) is given by

$$\mu_m \frac{d}{dx}\psi_{g,m}(x) + \sigma_{tg}^{j}\psi_{g,m}(x) = \frac{\chi_g}{2k_{eff}} \sum_{g'=1}^{G} \nu\sigma_{fg'}^{j} \sum_{n=1}^{N} \omega_n \psi_{g',n}(x) + \frac{1}{2} \sum_{g'=1}^{G} \sigma_{sj}^{g'\to g} \sum_{n=1}^{N} \omega_n \psi_{g',n}(x), \tag{3}$$

with $m = 1{:}N$, $g = 1{:}G$, $j = 1{:}J$ and $x_{j-1/2} \le x \le x_{j+1/2}$.

Equation (3) is a first-order ordinary differential equation with constant coefficients. In this paper, we use an iterative process to obtain a numerical solution of Eq. (3) with boundary conditions given by Eq. (2). To this end, we develop a nodal methodology in which we approximate the fission term in quadratic polynomial expansion.

2.3. Approximation of the fission term in quadratic polynomial expansion

The fission term is approximated by second-degree polynomial expansion

$$\frac{\chi_g}{2k_{eff}} \sum_{g'=1}^{G} \nu\sigma_{fg'}^{j} \sum_{n=1}^{N} \omega_n \psi_{g',n}(x) \cong a_{g,0}^{j} + a_{g,1}^{j} f_1^{j}(x) + a_{g,2}^{j} f_2^{j}(x), \tag{4}$$

where $f_1^{j}(x) = \frac{2}{h_j}(x - x_j)$ and $f_2^{j}(x) = \frac{1}{2}\left\{3\left[\frac{2}{h_j}(x - x_j)\right]^2 - 1\right\}$ are orthogonal polynomials, with $x_j = \frac{x_{j-1/2} + x_{j+1/2}}{2}$. The coefficients $a_{g,0}^{j}$, $a_{g,1}^{j}$, and $a_{g,2}^{j}$ are written as follows

$$a_{g,0}^{j} = \frac{\chi_g}{2k_{eff}} \sum_{g'=1}^{G} \nu\sigma_{fg'}^{j} \sum_{n=1}^{N} \omega_n \bar{\psi}_{g',n}^{j}, \tag{5}$$

$$a_{g,1}^{j} = \frac{\chi_g}{4k_{eff}} \sum_{g'=1}^{G} \nu\sigma_{fg'}^{j} \sum_{n=1}^{N} \omega_n \left[\psi_{g',n}\left(x_{j+1/2}\right) - \psi_{g',n}\left(x_{j-1/2}\right)\right], \tag{6}$$

$$a_{g,2}^{j} = \frac{\chi_g}{4k_{eff}} \sum_{g'=1}^{G} \nu\sigma_{fg'}^{j} \sum_{n=1}^{N} \omega_n \left[\psi_{g',n}\left(x_{j+1/2}\right) + \psi_{g',n}\left(x_{j-1/2}\right) - 2\bar{\psi}_{g',n}^{j}\right]. \tag{7}$$

Observation. To determine Eq. (5), the averaging operator $\frac{1}{h_j}\int_{x_{j-1/2}}^{x_{j+1/2}}(\cdot)\boldsymbol{dx}$ is applied in Eq. (4) and to obtain Eqs. (6) and (7), it is sufficient to consider, in Eq. (4), $\boldsymbol{x = x_{j-1/2}}$ and $\boldsymbol{x = x_{j+1/2}}$.

2.4. General solution of the system of equations

Equation (3), with the approximation of the fission term imposed in Eq. (4), takes the form

$$\mu_m \frac{d}{dx}\psi_{g,m}(x) + \sigma_{tg}^{j}\psi_{g,m}(x) - \frac{1}{2}\sum_{g'=1}^{G}\sigma_{sj}^{g'\to g}\sum_{n=1}^{N}\omega_n\psi_{g',n}(x) = a_{g,0}^{j} + a_{g,1}^{j}f_1^{j}(x) + a_{g,2}^{j}f_2^{j}(x). \tag{8}$$

The general solution of Eq. (8) can be written as follows

$$\psi_{g,m}(x) = \psi_{g,m}^{hom}(x) + \psi_{g,m}^{part}(x), \tag{9}$$

where $\psi_{g,m}^{hom}(x)$ is the homogeneous solution and $\psi_{g,m}^{part}(x)$ is a particular solution given by

$$\psi_{g,m}^{hom}(x) = \sum_{l=1}^{N\cdot G} \alpha_l^{j}\, a_{g,m}^{j}\left(\nu_l^{j}\right) exp\{-\nu_l^{j}\left(x - x_j\right)\}, \tag{10}$$

$$\psi_{g,m}^{part}(x) = b_{g,0m}^{j} + b_{g,1m}^{j} f_1^{\,j}(x) + b_{g,2m}^{j} f_2^{\,j}(x), \tag{11}$$

with $m = 1{:}N$, $g = 1{:}G$, $j = 1{:}J$ and $x \in \Gamma_j$.

To determine the coefficients $b_{g,0m}^{j}$, $b_{g,1m}^{j}$ and $b_{g,2m}^{j}$, it is sufficient to substitute the particular solution given in Eq. (11) in Eq. (8). In this way, by the equality of polynomials, we obtain, for $m = 1{:}N$, $g = 1{:}G$ and $j = 1{:}J$,

$$\begin{cases} \sigma_{tg}^{j} b_{g,2m}^{j} - \dfrac{1}{2} \displaystyle\sum_{g'=1}^{G} \sigma_{sj}^{g' \to g} \sum_{n=1}^{N} \omega_n b_{g',2n}^{j} = a_{g,2}^{j}, \\ \sigma_{tg}^{j} b_{g,1m}^{j} - \dfrac{1}{2} \displaystyle\sum_{g'=1}^{G} \sigma_{sj}^{g' \to g} \sum_{n=1}^{N} \omega_n b_{g',1n}^{j} = a_{g,1}^{j} - \left(6\mu_m / h_j\right) b_{g,2m}^{j}, \\ \sigma_{tg}^{j} b_{g,0m}^{j} - \dfrac{1}{2} \displaystyle\sum_{g'=1}^{G} \sigma_{sj}^{g' \to g} \sum_{n=1}^{N} \omega_n b_{g',0n}^{j} = a_{g,0}^{j} - \left(2\mu_m / h_j\right) b_{g,1m}^{j}. \end{cases} \tag{12}$$

Let $\boldsymbol{b}_{g,0}^{j} = (b_{g,0m}^{j})$, $\boldsymbol{b}_{g,1}^{j} = (b_{g,1m}^{j})$ and $\boldsymbol{b}_{g,2}^{j} = (b_{g,2m}^{j})$ be the order vectors $M = N \cdot G$ formed, in this order, by the coefficients $b_{g,0m}^{j}$, $b_{g,1m}^{j}$ and $b_{g,2m}^{j}$, $m = 1{:}N$, $g = 1{:}G$ and $C = (c_{mn})$ the order matrix M given by

$$c_{mn} = \begin{cases} \sigma_{tg}^{j} - \dfrac{1}{2} \displaystyle\sum_{g'=1}^{G} \sigma_{sj}^{g' \to g} \sum_{n=1}^{N} \omega_n \,, & m = n, \\ -\dfrac{1}{2} \displaystyle\sum_{g'=1}^{G} \sigma_{sj}^{g' \to g} \sum_{n=1}^{N} \omega_n \,, & m \neq n. \end{cases} \tag{13}$$

From Eqs. (12) and (13), one can write

$$\boldsymbol{b}_{g,2}^{j} = C^{-1} * \tilde{\boldsymbol{a}}_{g,2}^{j}, \tag{14}$$

$$\boldsymbol{b}_{g,1}^{j} = C^{-1} * \tilde{\boldsymbol{a}}_{g,1}^{j}, \tag{15}$$

$$\boldsymbol{b}_{g,0}^{j} = C^{-1} * \tilde{\boldsymbol{a}}_{g,0}^{j}, \tag{16}$$

where $\tilde{\boldsymbol{a}}_{g,2}^{j}$=$(a_{g,2}^{j})$, $\tilde{\boldsymbol{a}}_{g,1}^{j} = \left(a_{g,1}^{j} - \left(6\mu_m/h_j\right)b_{g,2m}^{j}\right)$ and $\tilde{\boldsymbol{a}}_{g,0}^{j} = (a_{g,0}^{j} - (2\mu_m/h_j)b_{g,1m}^{j}$ has order M, for $m = 1{:}N$, $g = 1{:}G$ and $j = 1{:}J$.

Substituting the homogeneous solution form $a_{g,m}^{j}(\nu_l^j)exp\{-\nu_l^j(x - x_j)\}$ into Eq. (8), we obtain the eigenvalue problem

$$\frac{1}{\mu_m}\sum_{g'=1}^{G}\sum_{n=1}^{N}\left(\sigma_{tg'}^{j}\delta_{gg'}\delta_{mn} - \sigma_{sj}^{g'\to g}\frac{\omega_n}{2}\right)a_{g',n}^{j}(\nu_l^j) = \nu_l^j \cdot a_{g,m}^{j}(\nu_l^j), \tag{17}$$

here δ_{mn} is the Kronecker delta given by $\delta_{mn} = \begin{cases}1, & m = n,\\ 0, & m \neq n.\end{cases}$ The variables ν_l^j are the eigenvalues and $a_{g,m}^{j}(\nu_l^j)$ are the components of the eigenvectors, with $m = 1{:}N$, $g = 1{:}G$, $j = 1{:}J$ and $l = 1{:}M$.

It is assumed that the angular fluxes of neutrons incident on the boundaries of the node Γ_j are known. Then, in Eq. (9), we consider $x = x_{j-1/2}$ when $g = 1{:}G$ and $m = 1{:}N/2$ and $x = x_{j+1/2}$ when $g = 1{:}G$ and $m = (N/2 + 1){:}N$. Hence, we obtain the system of linear and algebraic equations of order $M = N \cdot G$ given by

$$\sum_{l=1}^{M}\left[a_{g,m}^{j}(\nu_l^j)exp\{\nu_l^j(\nu_l^j h_j/2)\}\right]\alpha_l^j = \psi_{g,m}(x_{j-1/2}) - \psi_{g,m}^{part}(x_{j-1/2}), \tag{18}$$

for $m = 1{:}\,N/2$, $g = 1{:}\,G$ and $\psi_{g,m}^{part}(x_{j-1/2}) = b_{g,0m}^{j} - b_{g,1m}^{j} + b_{g,2m}^{j}$,

$$\sum_{l=1}^{M}[a_{g,m}^{j}(v_l^j)exp\{-v_l^j(v_l^j h_j/2)\}]\alpha_l^j = \psi_{g,m}(x_{j+1/2}) - \psi_{g,m}^{part}(x_{j+1/2}), \tag{19}$$

for $m = (N/2+1){:}\,N$, $g = 1{:}\,G$ and $\psi_{g,m}^{part}(x_{j+1/2}) = b_{g,0m}^{j} + b_{g,1m}^{j} + b_{g,2m}^{j}$.

2.5. Sweep equations

Figure 2 shows the angular fluxes at a node Γ_j in a group g of energy for S_4. The emergent angular fluxes are represented by $\psi_{g,3}^{j-1/2,em}$, $\psi_{g,4}^{j-1/2,em}$, $\psi_{g,1}^{j+1/2,em}$ and $\psi_{g,2}^{j+1/2,em}$, the incident angular fluxes are represented by $\psi_{g,1}^{j-1/2,in}$, $\psi_{g,2}^{j-1/2,in}$, $\psi_{g,3}^{j+1/2,in}$ and $\psi_{g,4}^{j+1/2,in}$ and in the internal part of the node are represented the average angular fluxes $\bar{\psi}_{g,1}^{j}$, $\bar{\psi}_{g,2}^{j}$, $\bar{\psi}_{g,3}^{j}$ and $\bar{\psi}_{g,4}^{j}$.

Figure 2: Angular fluxes at node $\boldsymbol{\Gamma_j}$ for S_4.

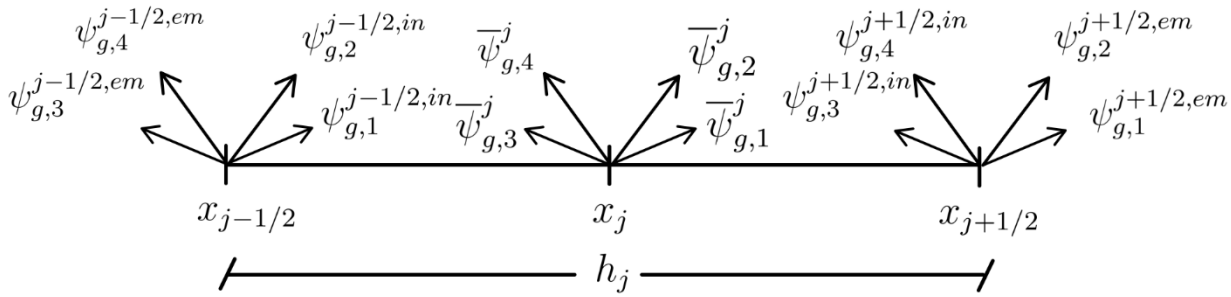

The sweep equations are used to obtain the angular fluxes emerging at the node faces, and for $g = 1{:}\,G$ and $j = 1{:}\,J$ they are given by

$$\psi_{g,m}(x_{j-1/2}) = \sum_{l=1}^{M}\alpha_l^j a_{g,m}^{j}(v_l^j)exp\{v_l^j h_j/2\} + \psi_{g,m}^{part}(x_{j-1/2}), \tag{20}$$

when $m = (N/2\ +\ 1){:}\,N$, and

$$\psi_{g,m}(x_{j+1/2}) = \sum_{l=1}^{M} \alpha_l^j a_{g,m}^j(\nu_l^j) exp\{-\nu_l^j h_j/2\} + \psi_{g,m}^{part}(x_{j+1/2}), \tag{21}$$

when $m = 1{:}\,N/2$.

2.6. Numerical solution (iterative process)

The iterative process is divided into two parts: an internal process, which aims to obtain successive estimates of the angular fluxes of neutrons emerging from homogeneous regions in the entire spatial domain, and an outer process, which obtains successive estimates of the fission source and k_{eff}, using the power method.

Internal iterative process. The spatial domain D is traversed initially from left to right (Fig. 1), starting at $\mathbf{\Gamma_1}$ (x = 0 cm) and ending at $\mathbf{\Gamma_J}$ (x = H cm) and then from right to left, starting at $\mathbf{\Gamma_J}$ and ending at $\mathbf{\Gamma_1}$, calculating the fluxes emerging from each homogeneous region in the scanning direction.

In the left-to-right direction, the coefficients α_l^j are obtained through Eqs. (18) and (19), considering the most recent estimates of the angular fluxes of neutrons incident on the left face of the node. Once this is done, the emergent fluxes of each node, $\psi_{g,m}^{j+1/2,em}$, are calculated using Eq. (21). When the process starts from right to left, the coefficients α_l^j are updated again and the emergent angular fluxes at the left interface of each node, $\psi_{g,m}^{j-1/2,em}$, are calculated using Eq.(20).

For the inner iterations, the convergence criterion in the scalar neutron flux is used

$$max\left|\frac{\phi_{gj}^{(i+1)} - \phi_{gj}^{(i)}}{\phi_{gj}^{(i+1)}}\right| \leq \varepsilon_1, \qquad j = 1{:}\,J+1 \; and \; g = 1{:}\,G, \tag{22}$$

where $\phi_{gj}^{(i)}$ represents the i-th estimate of the scalar neutron flux at the faces of node Γ_j and ε_1 is the precision imposed for the inner process.

Outer iterative process. The outer iterative process occurs as soon as the convergence criterion of the internal iterative process is met and aims to calculate the effective multiplication factor $(\boldsymbol{k_{eff}})$ using the expression

$$k_{eff}^{(p)} = k_{eff}^{(p-1)} \frac{\sum_{g'=1}^{G} \left\{ \sum_{j=1}^{J} h_j \nu \sigma_{fg'}^{j} \left[\frac{1}{2} \sum_{n=1}^{N} \omega_n \bar{\psi}_{g',n}^{j,(p)} \right] \right\}}{\sum_{g'=1}^{G} \left\{ \sum_{j=1}^{J} h_j \nu \sigma_{fg'}^{j} \left[\frac{1}{2} \sum_{n=1}^{N} \omega_n \bar{\psi}_{g',n}^{j,(p-1)} \right] \right\}}, \tag{23}$$

where the mean angular flux is given by

$$\bar{\boldsymbol{\psi}}_{\boldsymbol{g,m}}^{\boldsymbol{j}} = \sum_{\boldsymbol{l=1}}^{\boldsymbol{M}} \boldsymbol{\alpha}_{\boldsymbol{l}}^{\boldsymbol{j}} \boldsymbol{a}_{\boldsymbol{g,m}}^{\boldsymbol{j}} (\boldsymbol{\nu}_{\boldsymbol{l}}^{\boldsymbol{j}}) \frac{\mathbf{2}}{\boldsymbol{h_j \nu}_{\boldsymbol{l}}^{\boldsymbol{j}}} \mathbf{sinh}(\boldsymbol{\nu}_{\boldsymbol{l}}^{\boldsymbol{j}} \boldsymbol{h_j}/\mathbf{2}) + \boldsymbol{b}_{\boldsymbol{g,0m}}^{\boldsymbol{j}}.$$

For the outer iterations, two conditions are required: a convergence criterion in the mean scalar neutron flux at the nodes, represented by

$$max \left| \frac{\bar{\phi}_{gj}^{(p)} - \bar{\phi}_{gj}^{(p-1)}}{\bar{\phi}_{gj}^{(p)}} \right| \leq \varepsilon_2, \qquad j = 1{:}J \; and \; g = 1{:}G, \tag{24}$$

and a criterion for $\boldsymbol{k_{eff}}$ described by

$$\left| \frac{{k_{eff}}^{(p)} - {k_{eff}}^{(p-1)}}{{k_{eff}}^{(p)}} \right| \leq \varepsilon_3, \tag{25}$$

where $\boldsymbol{\varepsilon_2}$ and $\boldsymbol{\varepsilon_3}$ are the precisions imposed on the outer process.

3. NUMERICAL RESULTS

Numerical results are presented on a model-problem which was used to verify the accuracy of the nodal methodology proposed in this paper. These numerical results were compared with those of the DD fine mesh method. The Percentage Relative Deviation is given by PRD(%) = [(r^* - r)/r]*100, where r^* are the results of the methodology proposed in this paper and r are the results of the DD reference. The numerical algorithms of the proposed methodology and of the DD method were implemented in the MATLAB. The computer used to generate the results was a Samsung with an Intel Core i5-1135G7 processor, 2.4GHz with 8GB of RAM and a 64-bit Windows 11 operating system.

3.1. Model-Problem

The model-problem is a geometric configuration of the central line (on the horizontal) on Figure 3, that represents an ADS [7,8] type reactor with a one-dimensional domain on 389.76 cm having 13 regions with 7 material zones. The order of the Gauss-Legendre quadrature is N = 4 and neutrons with 4 energy groups were used. The left and right boundary conditions are vacuum.

Figure 3: 1D Configuration of sub-critical system (a = 18.56 cm).

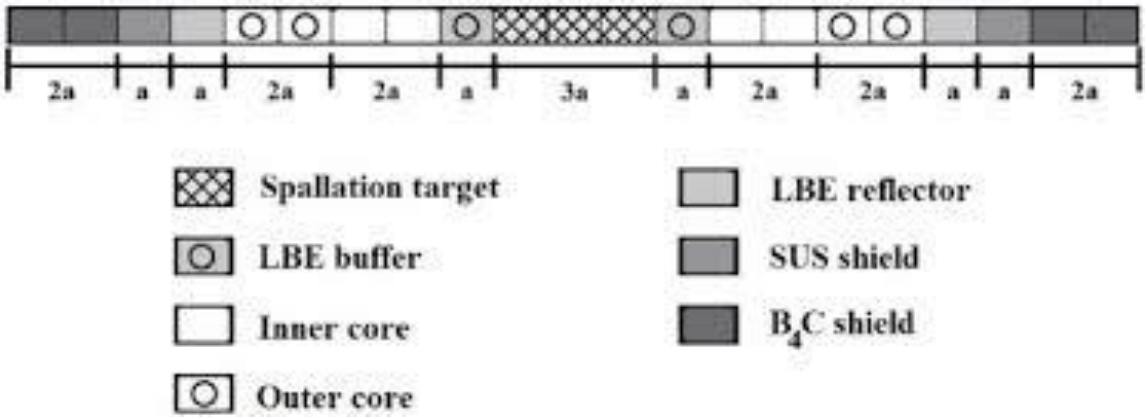

Source: Reference [7].

The fission spectrum used is given in Table 1.

Table 1: Fission spectrum.

χ_g			
$g = 1$	$g = 2$	$g = 3$	$g = 4$
0.86614323783790	0.11053026089759	0.22801119041383e-1[a]	0.52538222314407e-3

[a]Read as 0.22801119041383 x 10^{-1}.

The total macroscopic cross sections, the fission macroscopic cross sections and the differential scattering cross sections are given, respectively, in Tables 2, 3 and 4.

Table 2: Total macroscopic cross sections (cm^{-1}).

ZONE	σ_t^g			
	$g = 1$	$g = 2$	$g = 3$	$g = 4$
1	0.16646755622620	0.20708678925174	0.30141549207271	0.31932734589886
2	0.21453781478684	0.25592366410894	0.36732369116619	0.73085372516866
3	0.21727458632097	0.25535512674919	0.36455050492276	0.73119034416605
4	0.25058447457641	0.30112795045951	0.44160469618765	0.80050229238996
5	0.25841177609114	0.40242028424501	0.50955628791776	0.67905932681244
6	0.20837148400182	0.27296874233007	0.37203732809505	0.44393045088137
7	0.20808473120670	0.27235341988672	0.37190271311542	0.44246262690578

Table 3: Macroscopic fission cross sections (cm-1).

ZONE	$\nu\sigma_f^g$			
	$g = 1$	$g = 2$	$g = 3$	$g = 4$
1	0.00000000000000	0.00000000000000	0.00000000000000	0.00000000000000
2	0.00000000000000	0.00000000000000	0.00000000000000	0.00000000000000
3	0.00000000000000	0.00000000000000	0.00000000000000	0.00000000000000
4	0.00000000000000	0.00000000000000	0.00000000000000	0.00000000000000
5	0.00000000000000	0.00000000000000	0.00000000000000	0.00000000000000
6	0.10863339654228e-1[a]	0.32471096785577e-2	0.30006825711972e-2	0.49687562915774e-2
7	0.11221000361185e-1	0.42669203492471e-2	0.41451001694494e-2	0.69994284675514e-2

[a]Read as 0.10863339654228 x 10^{-1}.

Table 4: Isotropic differential scattering cross section (cm-1).

ZONE	$\sigma_s^{g' \to g}$				
	$g' \to g$	$g' = 1$	$g' = 2$	$g' = 3$	$g' = 4$
1	$g = 1$	0.16222913513400e+0[a]	0.00000000000000e+0	0.00000000000000e+0	0.00000000000000e+0
	$g = 2$	0.36697017471314e-2	0.20593424121073e+0	0.00000000000000e+0	0.00000000000000e+0
	$g = 3$	0.48715452703277e-3	0.10488387103767e-2	0.30110171532229e+0	0.00000000000000e+0
	$g = 4$	0.78964654747121e-5	0.00000000000000e+0	0.20161301186285e-3	0.31902446488107e+0
2	$g = 1$	0.20153835505666e+0	0.00000000000000e+0	0.00000000000000e+0	0.00000000000000e+0
	$g = 2$	0.10707621263452e-1	0.25128695243305e+0	0.00000000000000e+0	0.00000000000000e+0
	$g = 3$	0.17039929923862e-2	0.42768389582139e-2	0.36513472392174e+0	0.00000000000000e+0
	$g = 4$	0.10340815843129e-3	0.95415164020803e-6	0.15806435775153e-2	0.72871342075639e+0
3	$g = 1$	0.20467386504769e+0	0.00000000000000e+0	0.00000000000000e+0	0.00000000000000e+0
	$g = 2$	0.10227580563091e-1	0.25095710445471e+0	0.00000000000000e+0	0.00000000000000e+0
	$g = 3$	0.17256163669521e-2	0.40410598407383e-2	0.36241749462944e+0	0.00000000000000e+0
	$g = 4$	0.10549007331644e-3	0.76680706694453e-6	0.15365658856520e-2	0.72897305642182e+0
4	$g = 1$	0.23668102448269e+0	0.00000000000000e+0	0.00000000000000e+0	0.00000000000000e+0
	$g = 2$	0.11409522450233e-1	0.29606851516865e+0	0.00000000000000e+0	0.00000000000000e+0
	$g = 3$	0.18919368439678e-2	0.46707832812833e-2	0.43899130539522e+0	0.00000000000000e+0
	$g = 4$	0.11520982936293e-3	0.17936202249794e-5	0.19655013153264e-2	0.79794514657930e+0
5	$g = 1$	0.22549134074260e+0	0.00000000000000e+0	0.00000000000000e+0	0.00000000000000e+0
	$g = 2$	0.27709282726362e-1	0.35435686876018e+0	0.00000000000000e+0	0.00000000000000e+0
	$g = 3$	0.61981887073257e-3	0.34806523475536e-1	0.47151479865429e+0	0.00000000000000e+0
	$g = 4$	0.35742069153492e-4	0.00000000000000e+0	0.80200321963827e-2	0.58953264092285e+0
6	$g = 1$	0.19221930911845e+0	0.00000000000000e+0	0.00000000000000e+0	0.00000000000000e+0
	$g = 2$	0.10537653634523e-1	0.26190751249875e+0	0.00000000000000e+0	0.00000000000000e+0
	$g = 3$	0.11077656386834e-2	0.73387880672224e-2	0.36285507185274e+0	0.00000000000000e+0
	$g = 4$	0.32924647172602e-4	0.71793891929223e-5	0.21448608660985e-2	0.42556160238916e+0
7	$g = 1$	0.19202385524166e+0	0.00000000000000e+0	0.00000000000000e+0	0.00000000000000e+0
	$g = 2$	0.10436734926051e-1	0.26139167019435e+0	0.00000000000000e+0	0.00000000000000e+0
	$g = 3$	0.10905947200017e-2	0.72032757041649e-2	0.36296181839921e+0	0.00000000000000e+0
	$g = 4$	0.31879405980967e-4	0.58552011947768e-5	0.22345523271838e-2	0.42498221836133e+0

[a]Read as 0.16222913513400 x 10^0.

The tolerances for the convergence criteria are: $\boldsymbol{\varepsilon_1 = 10^{-5}}$ (for the inner iterations), $\boldsymbol{\varepsilon_2 = 10^{-7}}$ (for the mean scalar fluxes of the outer iterations) and $\boldsymbol{\varepsilon_3 = 10^{-9}}$ (for the $\boldsymbol{k_{eff}}$ of the outer iterations).

In Table 5 we list the values of $\boldsymbol{k_{eff}}$ obtained in the proposed methodology for different spatial grids. To generate the results of the DD method we use a mesh of 4096 nodes per region.

Table 5: Effective multiplication factor (k_{eff}).

$\boldsymbol{\Lambda_n^a}$	$\boldsymbol{k_{eff}}$	Cpu Time ($\boldsymbol{s}$)	PRD(%)[b]
Λ_0	0.66094067	1	-3.67e-2[c]
Λ_1	0.66119507	3	1.77e-3
Λ_2	0.66118681	9	5.25e-4
Λ_4	0.66118277	60	-8.51e-5
Λ_8	0.66118276	1464	-8.73e-5
DD Method	0.66118334	178	

[a]$\Lambda_n = 2^n$ spatial nodes per region.

[b]Percentage relative deviation in relation to the DD method.

[c]Read as -3.67 x 10^{-2}.

It is noted that the largest percentagem relative deviation obtained for $\boldsymbol{k_{eff}}$ (Table 5) by the method developed in this paper was approximately 0.04% in relation to the reference value generated by the DD method in fine-mesh calculation.

Table 6 presents the values of the scalar neutron fluxes at the interfaces of the material regions of the model-problem. The proposed methodology was implemented with 1 node per region and 16 $\boldsymbol{(\Lambda_4)}$ nodes per region. We calculated the percentage relative deviation of the scalar neutron fluxes of the proposed methodology in relation to the DD method.

Table 6: Scalar neutron flux ($cm^{-2}\ s^{-1}$).

$x\ (cm)$	Group	DD	Λ_0^a	Λ_4
37.12	1	2.89586489e-2[b]	2.91227620e-2 (5.66e-1)[c]	2.89622630e-2 (1.24e-2)
	2	1.06932802e-2	1.07546160e-2 (5.73e-1)	1.06955258e-2 (2.10e-2)
	3	2.20229186e-3	2.21646165e-3 (6.43e-1)	2.20330586e-3 (4.60e-2)
	4	7.77277795e-6	7.84287692e-6 (9.01e-1)	7.78402037e-6 (1.44e-1)
315.52	1	7.31249335e-1	7.35422187e-1 (5.70e-1)	7.31285286e-1 (4.91e-3)
	2	1.57941245e-1	1.58812888e-1 (5.51e-1)	1.57952621e-1 (7.20e-3)
	3	3.62760023e-2	3.64976584e-2 (6.11e-1)	3.62803266e-2 (1.19e-2)
	4	4.56531615e-4	4.60091218e-4 (7.79e-1)	4.56601306e-4 (1.52e-2)

[a]$\Lambda_n = 2^n$ spatial nodes per region.

[b]Read as 2.89586489 x 10^{-2}.

[c]Percentage relative deviation in relation to DD method.

4. CONCLUDING REMARKS

This paper describes the implementation of a semi-analytical nodal (coarse mesh) deterministic methodology for obtaining numerical solutions to the eigenvalue problems based on neutron transport theory, in slab geometry, with isotropic scattering, using the discrete ordinates formulation S_N and the multigroup energy formulation. The proposed methodology uses a quadratic polynomial approximation in the fission term of the transport equation and keeps the scattering term without approximation.

The construction of the neutron transport equation and the internal and outer iterative processes used to obtain the numerical solution of the eigenvalue problems were shown. It

is observed that, due to the approximation made in the fission term, k_{eff} does not appear in Eq. (21), thus, once the eigenvalues and eigenvectors have been calculated, it is not necessary to calculate them again when k_{eff} is updated in the outer iterative process.

This methodology, despite not being free from spatial truncation error in one-dimensional calculations, did not compromise the accuracy of the results nor greatly increase the execution times of the computational simulations in the model problem used. Computational algorithms were implemented in MATLAB.

In the model-problem presented previously, the proposed methodology provided real eigenvalues, and they appeared pairwise symmetric. We obtained good results according to the Diamond Difference [5] reference, which was implemented with 4096 nodes per region in the model-problem. The refinement did not significantly increase the computational cost in terms of response time and brought our results closer to those of analytical solutions, ensuring accuracy, efficiency, and reliability. Furthermore, we obtained good results with only one node per region.

For future work, we propose the extension of this methodology to two-dimensional problems using the multigroup energy formulation. At the moment, we are conducting a study to evaluate the possibility of applying this methodology to criticality (eigenvalue) calculations, considering other types of multidimensional geometry, e.g., rectangular Cartesian, cylindrical etc.

ACKNOWLEDGMENTS

The authors thank the Multi-scale Particle Transport Laboratory (LABTRAN) at IPRJ/UERJ for technical support.

FUNDING

This research was carried out with the support of the Coordination for the Improvement of Higher Education Personnel - Brazil (CAPES) - Financing Code 001. Natália Pinheiro is supported by financial support from UESC (Santa Cruz State University) to research.

CONFLICT OF INTEREST

All authors declare that they have no conflicts of interest.

REFERENCES

[1] Lewis, E. E.; Miller, W. F. **Computational methods of neutron transport**. 2nd Edition, Wiley, New York, USA, 1993. ISBN 0-471-09245-2.

[2] Badruzzaman, A. Nodal methods in transport theory. **Advances in Nuclear Scienceand Technology**, 12 1990. in <https://www.osti.gov/biblio/443936>.

[3] Lawrence, R. D. Progress in nodal methods for the solution of the neutron diffusion and transport equations. **Progress in Nuclear Energy**, v. 17, p. 271-301, 1986.

[4] Barros, R. C.; Larsen, E. W. A numerical method for discrete ordinate problems of one-group slab geometry without spatial truncation error. **Nuclear Science and Engineering**, v. 104, p. 199-208, 1990.

[5] de Abreu, M. P. Métodos determinísticos livres de aproximações espaciais para a solução numérica dominante de problemas de autovalor multiplicativo na formulação de ordenadas discretas da teoria do transporte de nêutrons. Tese de Doutorado, COPPE/UFRJ, Rio de Janeiro, RJ, Brasil, 1996.

[6] Ramírez, S. Cálculos de criticalidade usando a equação de transporte de nêutrons multigrupo unidimensional na formulação das ordenadas discretas a partir da solução analítica local. Tese de Doutorado, IPRJ/UERJ, Nova Friburgo, RJ, Brasil, 2021.

[7] Salas, L. L.; Silva, F. C.; Martinez, A. S. A new point kinetics model for ADS-type reactor using the importance function associated to the fission rate as weight function. **Annals of Nuclear Energy**, v 190, p. 1-20, 2023.

[8] Tsujimoto, K.; Sasa, T.; Nishihara, K.; Oigawa, H.; Takano, H. Neutronics design for lead-bismuth cooled accelerator-driven system for transmutation of minor actinides. **Journal Nuclear Science and Technology**, v. 41, n. 1, p. 21-36, 2004.

LICENSE